Journal for ImmunoTherapy of Cancer

Oncolytic VSV-IL-2 has enhanced anticancer vaccination adjuvant abilities

Victor Mullins-Dansereau,[1,2,3] Marie-Lou Myre,[1,2,3] Angelina Bardoul,[1,2,3] Karen Geoffroy,[1,2,3] Marco J Rallo Pita,[1,2,3] Delphine Béland,[1,2,3] Kim Leclerc Desaulniers,[1,3] Dominic Guy Roy,[1,2,3] Marie-Claude Bourgeois-Daigneault [1,2,3]

To cite: Mullins-Dansereau V, Myre M-L, Bardoul A, *et al*. Oncolytic VSV-IL-2 has enhanced anticancer vaccination adjuvant abilities. *Journal for ImmunoTherapy of Cancer* 2025;**13**:e010570. doi:10.1136/jitc-2024-010570

► Additional supplemental material is published online only. To view, please visit the journal online (https://doi.org/10.1136/jitc-2024-010570).

Accepted 07 May 2025

[1]Centre Hospitalier de l'Université de Montréal research center (CRCHUM), Montreal, Quebec, Canada
[2]Département de Microbiologie, Université de Montréal, Montreal, Quebec, Canada
[3]Institut du Cancer de Montréal, Montreal, Quebec, Canada

Correspondence to
Dr Marie-Claude Bourgeois-Daigneault;
marie-claude.bourgeois-daigneault@umontreal.ca

ABSTRACT

Background Heterologous oncolytic virus prime-boost vaccination is emerging as a promising cancer immunotherapy to establish potent antitumor immunity. With their natural ability to specifically destroy cancer cells, oncolytic viruses also allow for direct oncolysis and our team has previously demonstrated that they can be used as vaccination adjuvants when co-administered with antigenic peptides. As such, adjuvant oncolytic virus vaccines can easily be tailored to target any antigen, which is particularly important in the context of personalized vaccines against patient-specific mutations. Here, we tested if oncolytic viruses engineered to express the immune-stimulating transgene interleukin-2 have improved vaccination adjuvant potential.

Methods For this proof-of-concept study, we generated an oncolytic vesicular stomatitis virus (VSV) variant (MD51) that encodes the T-cell activator cytokine interleukin-2 and measured its vaccination adjuvant potential in a heterologous virus immune boosting approach, 1 week after immune priming compared with the parental virus (also MD51). Tumor-free and B16F10-Ova tumor-bearing mice were vaccinated against the Ova peptide using either virus as adjuvants. The immune response induced by each vaccination regimen was assessed by flow cytometry to characterize antigen-specific CD8 T cells over time. Treatment efficacy was also measured.

Results Our data show that VSV-interleukin-2 is superior as a vaccine boosting adjuvant compared with the parental virus as it induces more antigen-specific CD8 T cells with enhanced effector functions that persist over time. VSV-interleukin-2 vaccination also improves tumor control and survival.

Conclusions Overall, we show that engineered oncolytic virus platforms, such as VSV-interleukin-2, have the potential to improve vaccination efficacy and treatment outcomes. Our findings deepen our understanding of the immune mechanisms underlying the use of oncolytic viruses as anticancer vaccination platforms and will allow for the development of a new generation of improved oncolytic virus vaccine adjuvants.

Trial registration number NCT02285816.

WHAT IS ALREADY KNOWN ON THIS TOPIC

⇒ Oncolytic viruses preferentially kill cancer cells, induce a strong inflammatory response at the tumor site and are effective vaccination adjuvants. Oncolytic virus variants that are modified to encode immune-stimulating transgenes exhibit increased pro-inflammatory capacities and often improve treatment efficacy. Interleukin-2 is a cytokine that plays a key role in the function of effector CD8 T cells.

WHAT THIS STUDY ADDS

⇒ Here, we demonstrate that using an oncolytic vesicular stomatitis virus (VSV) variant encoding the immune-stimulating transgene interleukin-2 as a vaccine boosting adjuvant improves antigen-specific immunity and outcomes. Our work also describes oncolytic VSV-interleukin-2, which is a novel virus.

HOW THIS STUDY MIGHT AFFECT RESEARCH, PRACTICE OR POLICY

⇒ This study shows for the first time that an oncolytic virus that is modified to encode an immune-stimulating transgene is a superior boosting adjuvant for anticancer vaccination. Overall, our study could lead to more effective personalized anticancer immunotherapies.

INTRODUCTION

Oncolytic viruses (OVs) are characterized by their capacity to preferentially target and kill cancer cells.[1] It is now established that OV infection within the tumor microenvironment triggers inflammation and induces antitumor immunity. As such, OVs are interesting candidates for cancer immunotherapy.[2 3] Novel strategies using OVs for cancer treatment include personalized anticancer vaccination.[4 5] One particularly promising avenue is to exploit OVs as anticancer vaccination platforms such as in a heterologous viral prime-boost approach in which two different viruses encoding the same tumor antigen are administered sequentially to prime and boost antitumor immunity. Multiple preclinical studies have established the potential of OVs as boosting agents in such regimens[6–11] and this strategy is currently undergoing clinical testing (NCT02285816).

Our group has recently demonstrated that OVs are as effective when used as vaccine adjuvants co-administered with peptide antigens as when they are genetically modified to encode antigens.[9] In this context, the virus boosts antigen-specific immunity, an effect that is not observed when injecting antigenic peptides without adjuvants. The main advantage of adjuvant OV vaccines is that they can be rapidly and easily adapted to any antigenic peptide without requiring virus modifications. Here, we aimed at further improving the efficacy of this adjuvant vaccine platform by using an engineered OV with enhanced immune-stimulating properties. Particularly, we co-administer the OV vaccine adjuvant with antigenic peptides as a vaccine boost, 1 week after immune priming. More specifically, we used an oncolytic (MD51)[12] vesicular stomatitis virus (VSV) variant encoding the cytokine interleukin-2 (IL-2). IL-2 is a key player for T-cell activity, as well as for the induction of potent and long-lasting memory responses. Importantly, IL-2 is clinically used for the treatment of renal cell carcinoma and melanoma and therefore has already been shown to be well tolerated by patients with cancer. Notably, multiple in-human trials have investigated the use of IL-2 as an adjuvant for anticancer vaccination.[13 14] While early results were promising, the systemic dose of IL-2 required to induce antigen-specific immunity resulted in severe toxicity and the approach was abandoned.[15]

As opposed to systemic administration of the cytokine, treatment using an IL-2-engineered OV would allow for in situ production within the tumor. We therefore tested whether an oncolytic VSV variant encoding IL-2 would have improved vaccine adjuvant abilities while maintaining a good safety profile. Our data show that VSV-IL-2, when used as a boosting agent, improves antitumor immunity, as well as therapeutic efficacy. This proof-of-concept study demonstrates the potential of engineered OV platforms as adjuvants for anticancer vaccination.

MATERIAL AND METHODS

Cell lines and culture

The Vero (African green monkey renal epithelium), B16F10 (murine melanoma) and 293T (human kidney epithelium) cell lines were obtained from the American Type Culture Collection. The B16F10-OVA and CTLL-2 cell lines were kindly gifted by Drs John Stagg and Walid Mourad, respectively (University of Montreal Hospital Research Center). 4T1, Vero, B16F10 and B16F10-OVA were cultured in Dulbecco's Modified Eagle's Medium (DMEM, Thermo Fisher 11995073, Waltham, Massachusetts, USA) and CTLL-2 cells were cultured in Roswell Park Memorial Institute-1640 media (Wisent 350–000 CL, Saint-Jean-Baptiste, QC, Canada). All culture media were supplemented with 10% fetal bovine serum (FBS) (Wisent 098–150, Saint-Jean-Baptiste, QC, Canada) and cells were maintained at 37°C with 5% CO_2.

Viral constructs and assays

All VSVs used in this study are attenuated oncolytic VSVMΔ51 variants (deleted for the methionine 51 of the matrix protein) of the Indiana strain.[12] The VSV-yellow fluorescent protein (YFP) has already been described.[16] As previously reported for YFP, as well as another transgene,[17] the murine IL-2 transgene was inserted between the G and L genes of the viral genome, a location that allows for potent transgene expression without affecting viral replication.[17] Viruses were propagated in Vero cells. The adenovirus used in this study (Ad-OVA) is an E2/E3 deleted human type 5 adenovirus that was described previously and was propagated in 293 T cells.[9 18]

VSV titers were measured by plaque assay. Briefly, infectious samples were serially diluted in serum-free DMEM, and monolayers of confluent Vero cells were infected for 1 hour prior to agarose overlay (agarose 1% in 10% FBS-supplemented DMEM). Cells were incubated overnight at 37°C with 5% CO_2 and plaques were counted the next day.

Cell viability assay

For Coomassie blue assays: cells were fixed for 1 hour at room temperature (RT) with a solution of 25% glacial acetic acid (Fisher Scientific A38-500, Waltham, Massachusetts, USA) and 75% methanol (Chaptec MNX2903, Montreal, QC, Canada) and then stained using the same fixative supplemented with 0.01% Coomassie brilliant blue (Bio-Rad 1610400, Hercules, California, USA) for 45 min. Plates were then washed with tap water and allowed to dry. Signal intensity was quantified by solubilizing the Coomassie blue with 1% sodium dodecyl sulfate (BioShop 151-21-3, Burlington, Ontario, Canada) and measuring the absorbance of the solution at 595 nm using a SpectraMax multimode plate reader (Molecular Devices, San Jose, California, USA).

For Resazurin assays: resazurin sodium salt (STEMCELL 62758-13-8, Vancouver, British Columbia, Canada) was dissolved in phosphate-buffered saline (PBS) (Thermo Fisher 14190–250, Waltham, Massachusetts, USA) at a concentration of 0.06 mg/mL and sterilized using a 0.22 µm syringe filter (Ultident 229751, Montreal, QC, Canada). The resazurin solution was then added 1:3 (V/V) to the cells and incubated at 37°C with 5% CO_2 for 5 hours and the fluorescent signal was quantified at 560/590 nm using an EnSight multimode plate reader (Perkin Elmer, Waltham, Massachusetts, USA).

ELISA

Sample preparation: for in vitro IL-2 measurements, B16F10 cells were infected at a multiplicity of infection (MOI) of 10 and infection supernatants were collected at the indicated time points. For in vivo experiments, blood and tumors were collected 24 hours post-virus treatment. Blood was drawn in untreated microtubes and left undisturbed for approximately 1 hour at RT. Serum was collected following a 10 min centrifugation at 1,000 g. Tumors were cut into pieces and incubated for 1 hour

at 4°C in RIPA buffer (Abcam ab156034, Cambridge, UK) supplemented with 10% glycerol (Fischer Scientific G33-1, Waltham, Massachusetts, USA) and protease inhibitors (Roche 11836153001, Basel, Switzerland). Samples were then centrifugated at 15,000 g for 10 min and supernatants were collected for IL-2 quantification.

IL-2 concentrations were quantified using the murine IL-2 DuoSet ELISA kit (R&D Systems DY402-05, Minneapolis, Minnesota, USA). To do so, EIA/RIA 96-well plates (Corning Inc CLS3590, Corning, New York, USA) were coated with the capture antibody (kit part # 840137) in PBS overnight. Wells were then blocked (1% bovine serum albumin (BSA) (Wisent 800–096-EG, Saint-Jean-Baptiste, QC, Canada) in PBS) for 1 hour. Samples and recombinant murine IL-2 standard (kit part # 840139) were diluted in reagent diluent (0.1% BSA, 0.05% Tween (Fisher Scientific BP337-100, Waltham, Massachusetts, USA) in tris-buffered saline) and plated for 2 hours followed by the addition of the detection antibody (kit part # 840138) for another 2 hours. Streptavidin-HRP (kit part # 893975) was added to wells for 20 min before being incubated with a TMB/E substrate solution (Millipore Sigma ES022, Burlington, Massachusetts, USA). Finally, the chromogenic reaction was arrested using a stop solution (DY994 R&D Systems Minneapolis, Minnesota, USA), and signal was quantified by a SpectraMax multimode plate reader at 450 nm. All incubation periods took place at room temperature and wells were washed (PBS, 0.05% Tween) and dried between each step.

Western blot

Splenocytes from C57BL/6 mice were stimulated with virus-conditioned media for 10 min at 37°C with 5% CO_2. Cells were then immediately lysed on ice using RIPA buffer (150 mM NaCl, 50 mM Tris, 12 mM sodium deoxycholate, 16 mM Triton X-100, 3.5 mM SDS) supplemented with protease and phosphatase inhibitors (Roche 4906837001, Basel, Switzerland). Cleared lysates were migrated on 10% acrylamide gels (Bio-Rad 1620115, Hercules, California, USA) and transferred onto nitrocellulose membranes (Bio-Rad 1620115, Hercules, California, USA). Membranes were blocked with 5% BSA for 1 hour prior to probing with rabbit anti-mouse signal transducer and activator of transcription (STAT)5 or rabbit anti-mouse Phospho-STAT5 antibodies (Tyr694) (Cell Signaling technology 94205S and 9359S, Danvers, Massachusetts, USA) followed by a goat anti-rabbit horseradish peroxidase (HRP)-conjugated secondary antibody (Thermo Fisher 31460, Waltham, Massachusetts, USA). The signal was detected using the Immobilon Forte Western HRP substrate (Millipore Sigma WBLUF0100, Burlington, Massachusetts, USA) and a Chemidoc imaging system (Bio-Rad, Hercules, California, USA).

CTLL-2 assay

CTLL-2 cells were incubated for 4 days with conditioned media from B16F10 cells infected with either VSV-YFP or VSV-IL-2 at an MOI of 10. Viral particles were removed from the conditioned media using 50 kDa centrifugation filter units (Sartorius 14558875, Göttingen, Germany). Cell viability was determined by flow cytometry (FACSymphony A3, BD Bioscience, Franklin Lake, New Jersey, USA) using a blue fixable live/dead dye (Thermo Fisher L23105, Waltham, Massachusetts, USA). Conditioned media from uninfected B16F10 cells supplemented with recombinant murine IL-2 (25 IU/mL) (PeproTech 212–12, Cranbury, New Jersey, USA) was used as a positive control.

In vivo tissue collection and processing for flow cytometry analysis

Blood was harvested from the right saphenous vein using EDTA-coated capillaries (Sarstedt 17.2113.150, Nümbrecht, Germany) and transferred into tubes containing blood collection buffer (2% FBS, 5 mM EDTA and 0.02% sodium azide (Millipore Sigma E9884 and S2002, Burlington, Massachusetts, USA) in PBS. Red blood cells were lysed using red blood cell (RBC) lysis buffer (0.83% NH_4CL (VWR BDH9208, Radnor, Pennsylvania, USA) in H_2O) for 10 min and immune cells were then resuspended in PBS supplemented with 2% FBS prior to flow cytometry experiments.

Spleen, tumor-draining lymph nodes (TdLNs) and tumors were harvested in fluorescent activated cell sorting (FACS) buffer (2% FBS, 0.01% sodium azide (Millipore Sigma, S2002, Burlington, Massachusetts, USA) in PBS) on ice. Spleens and TdLNs were mashed through a 70 µm cell strainers (Fisher Scientific 22-363-548, Waltham, Massachusetts, USA) and splenic red blood cells were lysed using RBC lysis buffer for 7 min prior to resuspension in FACS buffer.

Tumors were cut into small pieces and resuspended in tumor dissociation buffer (Miltenyi Biotec 130-096-730, Bergisch Gladbach, Germany) for 30 min at 37°C in 5% CO_2. Samples were then mashed using microtube pestles (Fisher Scientific FS7495101590, Waltham, Massachusetts, USA) and incubated for another 30 min at 37°C in 5% CO_2. Finally, lysates were filtered through 70 µm cell strainers and resuspended in FACS buffer.

Flow cytometry and antibodies

For intracellular cytokine expression, cells were stimulated ex vivo with Ova (SIINFEKL) or VSV-N (RGYVYQGL) peptides (1 µM) in RPMI-1640 supplemented with 10% FBS for 6 hours and GolgiStop (BD Bioscience 554724 Franklin Lakes, New Jersey, USA) was added after the first hour. Cells were stained for surface markers in FACS buffer, permeabilized using the BD Cytofix/Cytoperm Kit (BD Bioscience 554714, Franklin Lakes, New Jersey, USA) and then stained using corresponding antibodies. Data was acquired using a Symphony A3 flow cytometer (BD Bioscience, Franklin Lakes, New Jersey, USA) and analyzed with the FlowJo V.10.10.0 software (BD Bioscience, Franklin Lakes, New Jersey, USA).

Viability dye

LIVE/DEAD Fixable Yellow from Thermo Fisher Scientific.

Antibodies

CD3-SB702 (clone 17A2), CD4-BUV496 (clone RM4-5), CD25-SB645 (clone PC61.5), CD44-Alexa Fluor 700 (clone IM7), CD45-PE-eF610 (clone 30-F11), CD62L-BV786 (clone MEL-14), CD127-FITC (clone A7R34), KLRG1-APC-Cy7 (clone 2F1), PD-1-BUV396 (clone J43), IFNγ-APC (clone XMG1.2), IL-2-BV450 (clone JES6-5H4) and TNF-PE (clone MP6-XT22) were purchased from Thermo Fisher Scientific (Waltham, Massachusetts, USA), CD8-BV510 (clone 53–6.7) from BioLegend (San Diego, California, USA) and PD-1-BUV395 (CD279, clone 29F.1A12) from BD Biosciences (Franklin Lakes, New Jersey, USA).

Tetramers

Biotinylated H2-Kb Ova (257–264, SIINFEKL) and VSV-NP (52–59, RGYVYQGL) monomers were obtained from the NIH Tetramer Core (Emory University, Atlanta, Georgia, USA) and tetramerized in-house. Briefly, PE-conjugated or APC-conjugated (Thermo Fisher S866 and S868, Waltham, Massachusetts, USA) streptavidins were progressively added to the biotinylated major histocompatibility complex (MHC) monomers at a rate of 5 µL every 5 min for approximately 90 min. Following an overnight incubation at 4°C, tetramers were cleaned using 100 kDa centrifugal filter units (Millipore Sigma UFC510024, Burlington, Massachusetts, USA) and stored at 4°C.

In vivo experiments and tumor models

6–8 weeks old female C57BL/6 mice (Charles River, Wilmington, Massachusetts, USA) were used for all experiments.

Heterologous virus prime-boost vaccination: for immune priming, mice were injected intramuscularly in the quadriceps (50 µL/leg) with 10^8 infectious units of Ad-Ova or PBS as a control. For immune boosting, the mice were injected intravenously 7 days post-prime with 10^8 plaque-forming units (PFUs) of VSV-YFP or VSV-IL-2 premixed with 100 µg of ovalbumin (Ova) peptide (Biosynth POV 3659-PI, Staad Switzerland) or PBS as a

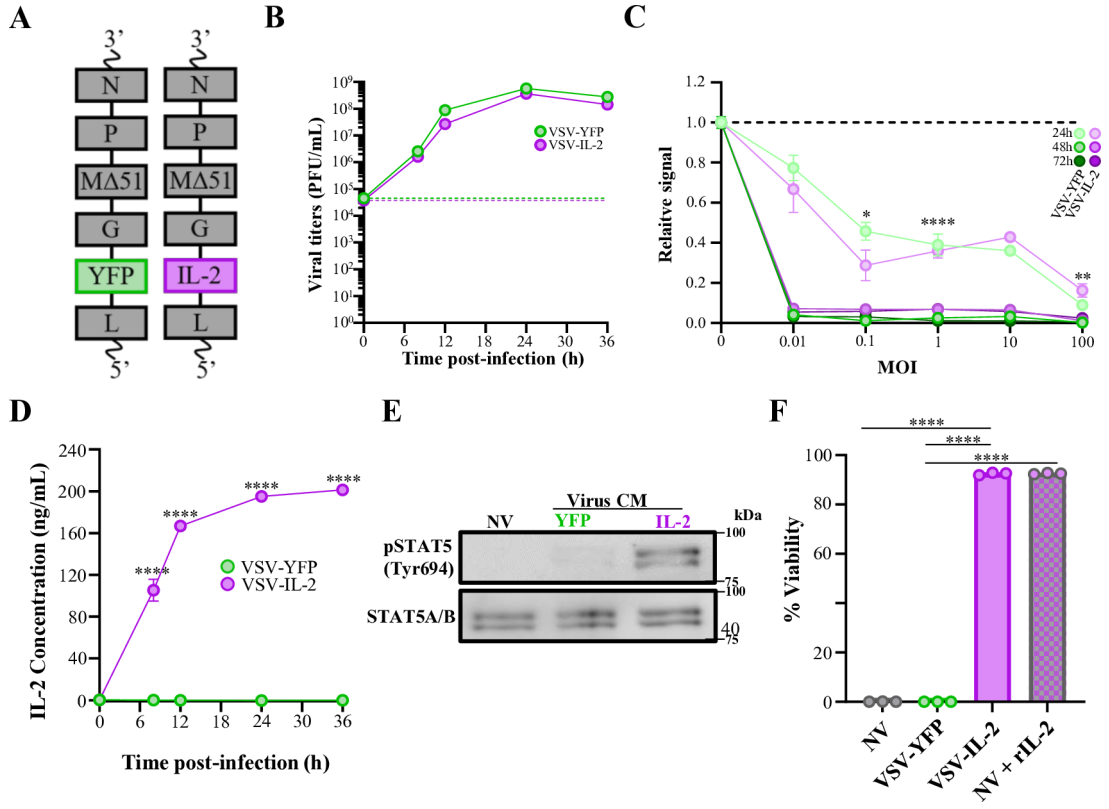

Figure 1 IL-2 is expressed and functional on VSV-IL-2 infection. (A) Schematic representation of the VSV-YFP and VSV-IL-2 viral genomes. (B) Viral growth curves of VSV-YFP and -IL-2 on infection of B16F10 cells at an MOI of 0.1 (n=5). The dashed lines represent viral inputs. (C) Relative viability of B16F10 cells infected for 24, 48 and 72 hours with VSV-YFP or -IL-2 at various MOIs as measured by Coomassie blue stain (n=6). (D) Concentrations of IL-2 in culture supernatants from B16F10 cells infected with VSV-YFP or -IL-2 at an MOI of 10 for various time points (n=3). (E) Western blot analysis of STAT5 and pSTAT5 from splenocytes stimulated with conditioned media (CM) from B16F10 cells infected with either VSV-YFP or VSV-IL-2 at an MOI of 10 for 10 min. (F) Percent viability of CTLL-2 cells cultured for 4 days with virus-cleared CM from B16F10 cells infected with either VSV-YFP or -IL-2 at an MOI of 10 or with uninfected B16F10 CM supplemented or not with recombinant IL-2 (rIL-2) (n=3). ****p≤0.0001. (Non-parametric t-test (B–D) and two-way analysis of variance with post hoc multiple comparison (F)). IL, interleukin; MOI, multiplicity of infection; STAT5, signal transducer and activator of transcription 5; pSTAT5, phosphorylated STAT5; VSV, vesicular stomatitis virus; YFP, yellow fluorescent protein.

control. For prophylactic experiments, the mice were challenged with 10^6 B16F10-Ova cells subcutaneously in the left flanks 100 days post-prime. For therapeutic experiments, B16F10-Ova tumors were seeded in the same location 1-week prior to immune priming. Immune characterization began 7 days post-boost as indicated in the corresponding figure legends.

Statistical analyses and reporting guidelines

Statistical analyses were performed using GraphPad Prism V.10.0.0 for Windows (Boston, Massachusetts, USA) as described in the figure legends. We used the ARRIVE guidelines V.2.0.

RESULTS

VSV-IL-2 has similar replicative and oncolytic abilities compared with the parental virus

First, we engineered the viral backbone of VSVMD51 to encode murine IL-2. To do so, we inserted the transgene between the viral G and L genes (figure 1A), a location that has been shown for other variants to allow for important amounts of transgene expression without impairing virus replication.[17] We then tested if this insertion affected virus replication. To do so, B16F10 mouse melanoma cells were infected with VSV-YFP or VSV-IL-2 at an MOI of 0.1 and virus production was assessed at various time points by plaque assay. We observed identical growth kinetics for both viruses (figure 1B), indicating similar replicative capacities. Cancer cell viability was also assessed as a readout of OV-mediated cancer killing. Once again, we observed comparable cell death from cells infected with VSV-IL-2 and VSV-YFP, with cell killing increasing over time with most MOIs showing viabilities of 0% at 48 hours post-infection (figure 1C and online supplemental figure 1A). Overall, our results show that the insertion of the *IL-2* transgene within the genome of VSV does not affect virus replication and cytotoxicity.

The *IL-2* transgene is expressed and functional on infection

Next, we sought to measure IL-2 expression following infection. To do so, B16F10 cells were infected with VSV-YFP or VSV-IL-2 at an MOI of 1 for 24 hours and IL-2 expression was assessed by flow cytometry. As expected, IL-2 was only detected in cells infected with VSV-IL-2 (online supplemental figure 1B). To measure IL-2 production, the cytokine was then quantified in culture supernatants by ELISA. As expected, we found that IL-2 was secreted by cells infected with VSV-IL-2, but not the parental virus (figure 1D). Notably, this production was shown to be robust as 100 ng/mL of IL-2 were detected from infected cells as early as 8 hours post-infection and a peak concentration of 200 ng/mL was reached within 24 hours. Next, we assessed the functionality of the virally-encoded IL-2 by measuring intracellular signaling following stimulation. On binding to its receptor, IL-2 engages a signaling cascade leading to the phosphorylation of STAT5.[19] We generated conditioned media from virus-infected B16F10 cells and used this media to stimulate splenocytes. Total and phosphorylated STAT5 (pSTAT5) levels were then measured by western blot. Our data show that while a weak band of pSTAT5 was detected for the parental virus, a clear increase was observed in cells stimulated with VSV-IL-2 conditioned medium and total levels of STAT5 remained constant in all conditions (figure 1E). To further confirm the functionality of IL-2, we exploited CTLL-2 cells, a CD8 T cell line that requires IL-2 for survival. CTLL-2 cells were exposed to either recombinant IL-2 (positive control) or conditioned media from VSV-YFP or VSV-IL-2-infected B16F10 cells for 4 days. To prevent cell death from virus infection, viral particles were filtered out of the conditioned media using centrifugation filters with a 50 kDa cut-off. Cell viability was assessed using trypan blue. Our data show more than 90% viability for cells cultured with VSV-IL-2 conditioned medium, which is similar to the recombinant IL-2 positive control, as opposed to the parental virus condition for which the cells were all dead (figure 1F). Similar findings were obtained when measuring total cell numbers (dead and alive) in the different conditions as a readout of proliferation (online supplemental figure 1C). Overall, our data show that VSV-IL-2 infection allows for the rapid and robust production of functional IL-2.

We next wanted to measure IL-2 concentrations in tumors on VSV-IL-2 infection. To do so, subcutaneous B16F10-Ova tumors were treated with single intravenous doses of 10^8 PFUs of VSV-YFP or VSV-IL-2 at days 14 post-implantation. We chose this experimental schedule and dose to recapitulate VSV heterologous prime-boost vaccines, the focus of this study.[9 18] Tumors and blood samples were collected 24 hours post-virus treatment and IL-2 concentrations were measured by ELISA. Consistent with transgene production after infection, IL-2 was detected in greater amounts in the samples from VSV-IL-2-treated mice compared with VSV-YFP (figure 2A). Interestingly, we also detected IL-2 in the circulation of VSV-IL-2-treated mice, although at lower concentrations compared with that of the tumors. In contrast, we could not detect IL-2 in the blood of VSV-YFP treated mice.

We next wanted to determine if VSV-IL-2 could confer therapeutic benefits as a monotherapy (without vaccination). In line with previous studies,[6 20] a single intravenous dose of the parental VSV-YFP virus did not confer therapeutic benefits in this VSV-resistant tumor model, and we did not observe any difference with VSV-IL-2 in this context (figure 2B). We next measured virus replication in tumors 24 hours post-virus treatment and found that both VSV-YFP and VSV-IL2 could replicate to similar levels in vivo (figure 2C).

Although we did not actively immunize the mice by using the virus as a vaccine adjuvant, VSV is known to induce antitumor immunity on its own.[20 21] We therefore measured the immune response induced by VSV-IL-2 treatment. First, we found that the circulating numbers of CD8 T cells were significantly increased at-week post-treatment with both viruses and this increase was similar

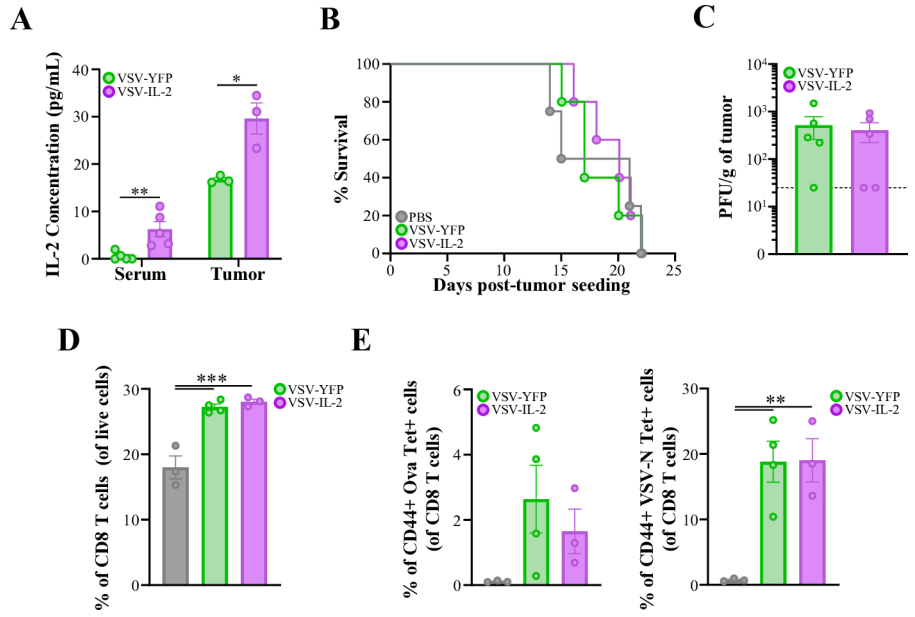

Figure 2 VSV-IL-2 monotherapy does not confer therapeutic benefits in the B16F10 tumor model. (A) IL-2 concentrations in the serum (n=5) and tumors (n=3) of B16F10-Ova subcutaneous tumor-bearing mice 24 hours post-VSV-YFP or VSV-IL-2 treatment as measured by ELISA. (B) Kaplan-Meier analysis of B16F10-Ova subcutaneous tumor-bearing mice treated with PBS (n=4) or a single intravenous injection of VSV-YFP (n=5) or VSV-IL-2 (n=5) on day 14. (C) Viral loads in tumors (n=5), (D) % CD8 T cells in the blood and (E) % Ova tet+ and VSV-tet+ (of CD8 T cells) in the blood 24 hours post-treatment with VSV-YFP or VSV-IL-2 (n=3 (PBS), 4 (VSV-YFP) and 3 (VSV-IL-2). *p≤0.05, **p≤0.01 ***p≤0.001. (Non-parametric t-test (A, E) and two-way analysis of variance with post hoc multiple comparison (D, E, F)). IL, interleukin; Ova, ovalbumin; PFUs, plaque forming units; VSV, vesicular stomatitis virus; YFP, yellow fluorescent protein.

for VSV-YFP and VSV-IL-2 (figure 2D). Since the tumors express the Ova antigen, we then used tetramers to detect Ova-specific, as well as VSV-specific CD8 T cells post-treatment and found, once again, that both viruses induced comparable responses (figure 2E). Interestingly, we did detect Ova-specific cells (2% of CD8 T cells) even in the absence of active vaccination and, as expected, both viruses induced strong VSV responses (almost 20% of CD8 T cells).

VSV-IL-2 boosting adjuvant vaccine improves antigen-specific immunity early after treatment

We next sought to evaluate the vaccine adjuvant potential of VSV-IL-2. We first tested the virus in a tumor-free setting. To do so, C57BL/6 mice were vaccinated against Ova using a heterologous viral prime-boost regimen. As described in figure 3A, the mice were first primed with Ad-Ova and boosted with either adjuvant VSV-YFP or VSV-IL-2 (both co-administered with the Ova peptide SIINFEKL) 7 days later. Immune characterization was done by flow cytometry 7 days post-boost and Ova tetramers (Ova Tet) were used to identify antigen-specific cells (see gating strategy in online supplemental figure 2A,B). We focused our analysis on CD8 T cells because the peptide we use for vaccination is MHC-I restricted.[22] As expected, only vaccinated mice had a clear population of circulating Ova-specific CD8 T cells (figure 3B). When quantifying the frequency of CD3+CD8+ T cells that were Ova Tet+, we found that mice vaccinated with VSV-IL-2 had 1.5 times more antigen-specific cells in comparison with mice vaccinated with VSV-YFP (figure 3C). We then further characterized the Ova-specific CD8 T cells and assessed their memory subsets using the markers CD44 and CD62L, which allow to identify effector memory (Tem, CD44+CD62L−), central memory (Tcm, CD44+CD62L+), as well as naïve (CD44−CD62L+) and double negative (DN, CD44−CD62L−) cells (see gating strategy in online supplemental figure 2C). Our results did not reveal differences in the proportions of the different memory subsets in mice from the different cohorts (figure 3D,E). We next investigated the memory and effector subsets of Ova-specific CD8 T cells using the KLRG1 and CD127 markers, which allow to identify short-lived effector (SLECs, KLRG1+CD127−), double-positive effector (DPECs, KLRG1+CD127+), memory precursor effector (MPECs, KLRG1−CD127+) and early effector (EECs, KLRG1−CD127−) cells (see gating strategy in online supplemental figure 2C). Interestingly, we found that VSV-IL-2 induced significantly more MPECs, compared with VSV-YFP (figure 3F,G).

We next assessed the effector functions of the Ova-specific cells induced by vaccination by measuring the production of the cytokines interferon (IFN)-γ and tumor necrosis factor (TNF)-α,[23] on antigen exposure. As expected, we observed that only CD8 T cells from Ova-vaccinated mice produced the cytokines on peptide stimulation (figure 4). Interestingly, we also observed significantly more IFN-γ+ and IFN-γ+TNF-α+ CD8 T cells with VSV-IL-2 vaccination. Taken together, our results

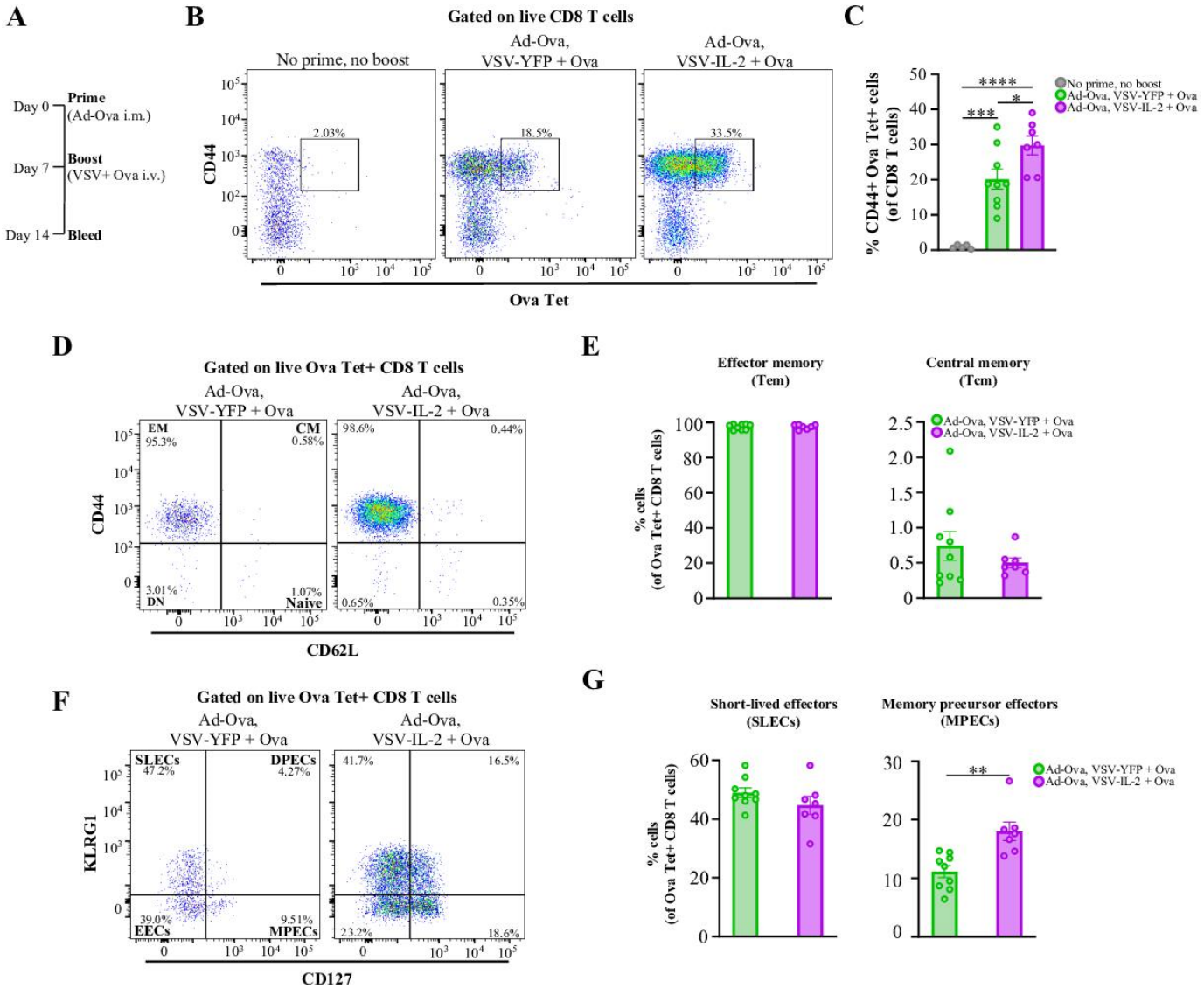

Figure 3 Adjuvant VSV-IL-2 boost enhances antigen-specific CD8 T cells and favors an MPEC profile early after vaccination. (A) Schematic representation of the timeline used for prophylactic vaccination. (B) Representative dot plots showing CD44+, Ova tetramer+CD8 T cells (CD3+CD8+) from the blood at day 14 of mice vaccinated with Ad-Ova and boosted 7 days later with adjuvant VSV-YFP or VSV-IL-2 (both co-administered with Ova peptides) and (C) percentage of CD44+, Ova Tet+effector T cells from all mice in the experiment (n=5 (PBS), 9 (VSV-YFP) and 7 (VSV-IL-2)). (D) Representative dot plots showing the expression of CD44 and CD62L by CD8 Ova Tet+cells from the same mice as in B, as well as the gating strategy to distinguish EM, CM, naïve and double-negative cells and (E) percentages of EM and CM Ova Tet+CD8 T cells from all mice in the experiment at day 14 post-prime (n=5 (PBS), 9 (VSV-YFP) and 7 (VSV-IL-2)). (F) Representative dot plots showing the expression of KLRG1 and CD127 by CD8 Ova Tet+cells from the different groups as well as the gating strategy to distinguish MPECs, SLECs, DPECs and EECs and (G) percentages of Ova Tet+CD8 T cells from each effector subset from all mice in the experiment (n=5 (PBS), 9 (VSV-YFP) and 7 (VSV-IL-2)). *p≤0.05, ***p≤0.001, ****p≤0.0001 (one-way analysis of variance with post hoc multiple comparison (E), non-parametric t-test (E, G)). CM, conditioned media; DPEC, double-positive effectors; EEC, early effector; EM, effector memory; IL, interleukin; i.m., intramuscular; i.v., intravenous; Ova, ovalbumin; PBS, phosphate-buffered saline; VSV, vesicular stomatitis virus; YFP, yellow fluorescent protein.

indicate that vaccination boost using VSV-IL-2 as an adjuvant is more effective compared with VSV-YFP.

We next sought to characterize the antigen-specific CD8 T cells over time. We thus repeated the experiment and collected blood samples at different time points. At day 100 post-prime, mice were challenged with subcutaneous B16F10-Ova cells. Tumor growth was also monitored (see timeline in figure 5A). We found that both VSV-YFP and VSV-IL-2 adjuvant vaccine boosts trigger long-lasting responses as more than 20% of CD8 T cells were still Ova-specific at 98 days post-prime (figure 5B). In comparison, the response induced against the virus was minimal and completely faded over time (online supplemental figure 4). We also observed that while we once again detected more Ova-specific CD8 T cells with VSV-IL-2 vaccination

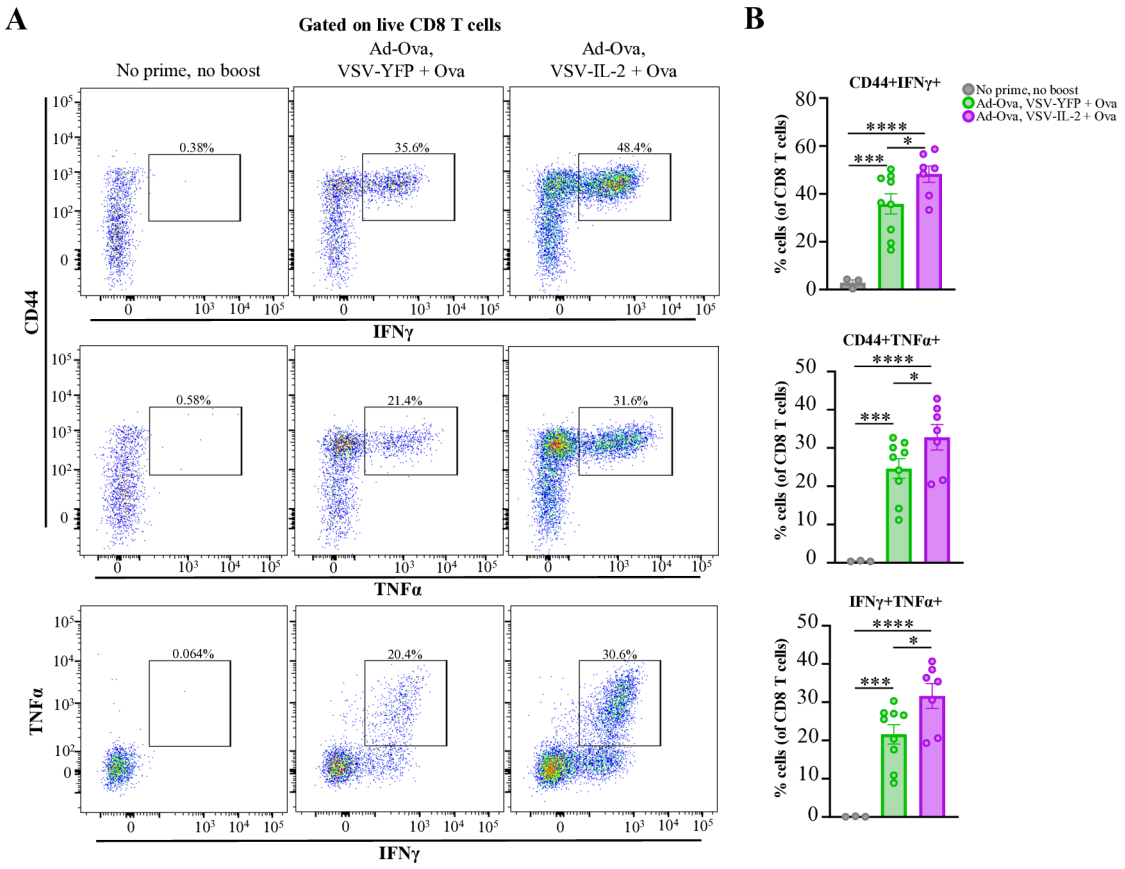

Figure 4 Adjuvant VSV-IL-2 vaccine boost improves the effector functions of Ova-specific CD8 T cells early after vaccination. (A) Representative dot plots showing the expression of CD44 and IFN-γ (top panels) or TNF-α (middle panels) or of both IFN-γ and TNF-α (bottom panels) by CD8 T cells following ex vivo stimulation of blood cells with Ova peptides 7 days post-boost and (B) percentages of CD44+IFN-γ+ (top panel), CD44+TNF-α+ (middle panel) or IFN-γ+TNF-α+ (bottom panel) CD8 T cells from all mice in the experiment at day 14 (n=3 (PBS), 9 (VSV-YFP) and 7 (VSV-IL-2)), *p≤0.05, ***p≤0.001, ****p≤0.0001 (one-way analysis of variance with post hoc multiple comparison (B)). IFN, interferon; IL, interleukin; Ova, ovalbumin; PBS, phosphate-buffered saline; TNF, tumor necrosis factor; VSV, vesicular stomatitis virus; YFP, yellow fluorescent protein.

early after vaccination, this difference was lost by day 42. Also, similar to what was observed 1 week after vaccination, Tem and Tcm frequencies were similar between groups over time (figure 5C). Notably, Tcm frequencies increased post-tumor challenge, but this increase was once again similar for both groups. The increase in MPECs that we observed with VSV-IL-2 at day 14 in our previous experiment was also observed here. This increase of KLRG1-CD127+cells, was maintained for up to day 126 with 5–15% more cells detected at all time points with adjuvant VSV-IL-2 boost (figure 5D). When assessing effector functions over time, we once again observed an increased production of effector cytokines with VSV-IL-2 14 days post-prime, but this difference was lost 28 days later (figure 5E).

Finally, when monitoring tumor growth, we observed that both vaccines could effectively slow tumor progression and extend survival to similar levels in this prophylactic setting (figure 5F,G). Taken together, our results show that immune boosting with adjuvant VSV-IL-2 vaccination promotes a long-lasting KLRG1−CD127+phenotype in antigen-specific CD8 T cells but fails at improving therapeutic benefits when animals are vaccinated 100 days prior to tumor challenge.

Therapeutic VSV-YFP and VSV-IL-2 adjuvant boost vaccines do not impact CD4 T-cell numbers or T-cell activation

Given that IL-2 can impact CD4 T cells, we next wanted to determine if CD4 T-cell numbers were different between VSV-YFP and VSV-IL-2 in the spleens, tumors and tumor-draining lymph nodes of vaccinated animals. To do so, we vaccinated B16F10-Ova tumor-bearing mice and collected tissues 7 days later for immune analysis (see timeline in figure 6A). We did not analyze Ova-specific CD4 T cells because our vaccine uses a CD8 T cell-specific peptide and would therefore not induce Ova-specific CD4 T-cell responses. Instead, we measured the activation of both CD4 and CD8 T cells by analyzing CD25 and programmed cell death 1 (PD-1) expression, two markers that are found at the surface of activated T cells.[24] Our data show increased percentages of immune cells (CD45+) in the tumors of vaccinated animals and no differences in CD4 or CD8 T-cell frequencies nor in their activation status

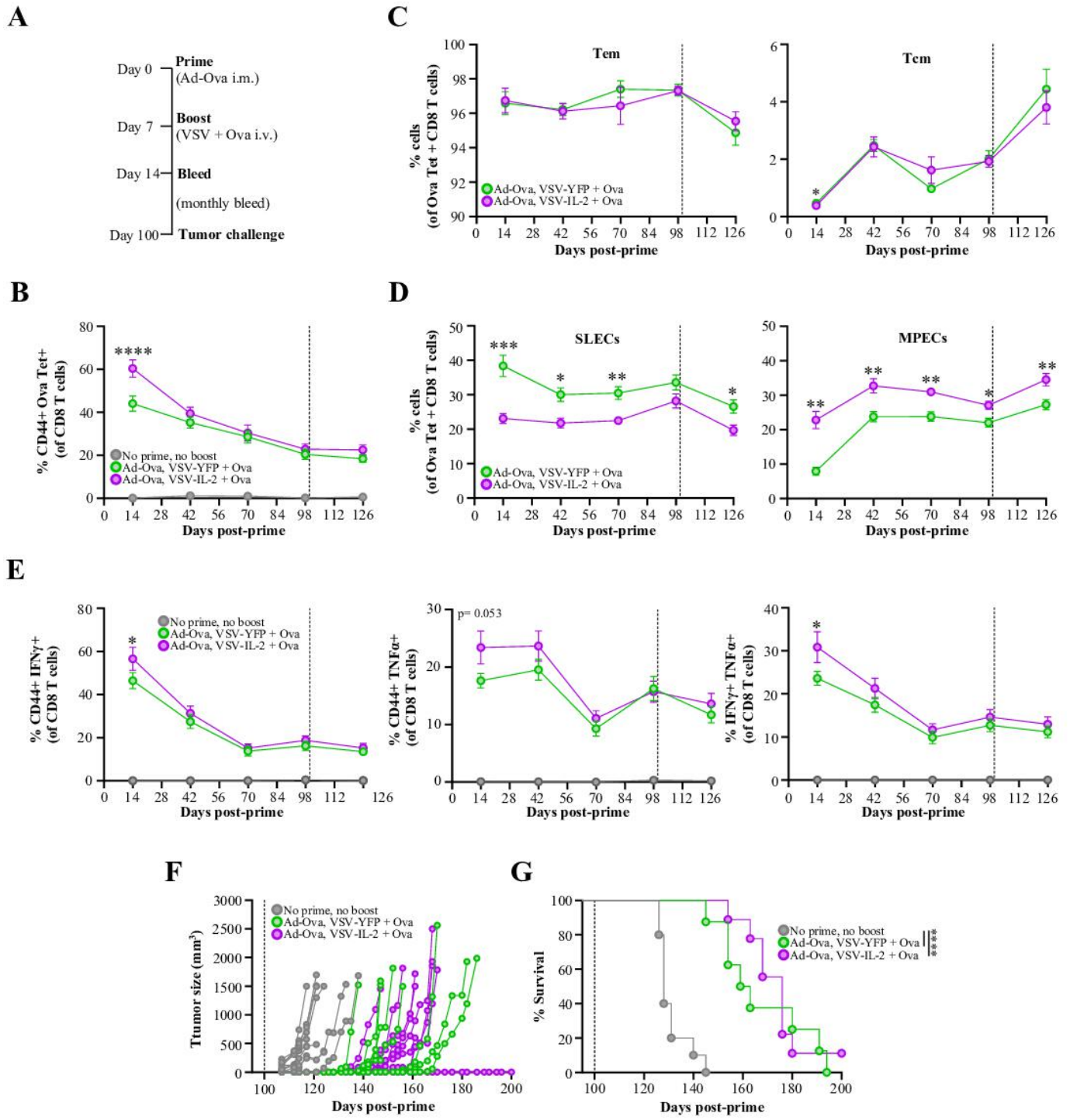

Figure 5 Adjuvant VSV-IL-2 boosting generates more antigen-specific MPECs and fewer SLECs compared with VSV-YFP. (A) Schematic representation of the timeline used in this figure (n=5 (PBS), 8 (VSV-YFP) and 9 (VSV-IL-2)). Kinetics of the frequencies of (B) CD44+Ova Tet+, (C) Ova-specific EM (CD44+CD62L–) and CM (CD44+CD62L+), (D) Ova-specific SLECs (KLRG1+CD127–) and MPECs (KLRG1–CD127+), (E) CD44+IFN-γ+, CD44+TNF-α+ or IFN-γ+TNF-α+ CD8 T cells from the blood following the ex vivo restimulation with Ova peptide. (F) Tumor growth curves and (G) Kaplan-Meier analysis of the vaccinated mice following subcutaneous B16F10 tumor challenge at day 100. *p≤0.05, **p≤0.01 ***p≤0.001, ****p≤0.0001 (two-way analysis of variance with post hoc multiple comparison (B, E), non-parametric t-test (C, D) and Mantel-Cox (G)). CM, conditioned media; EM, effector memory; IFN, interferon; IL, interleukin; i.m., intramuscular; i.v., intravenous; MPECs, memory precursor effector cell; Ova, ovalbumin; PBS, phosphate-buffered saline; SLECs, short-lived effector cell; TNF, tumor necrosis factor; VSV, vesicular stomatitis virus; YFP, yellow fluorescent protein.

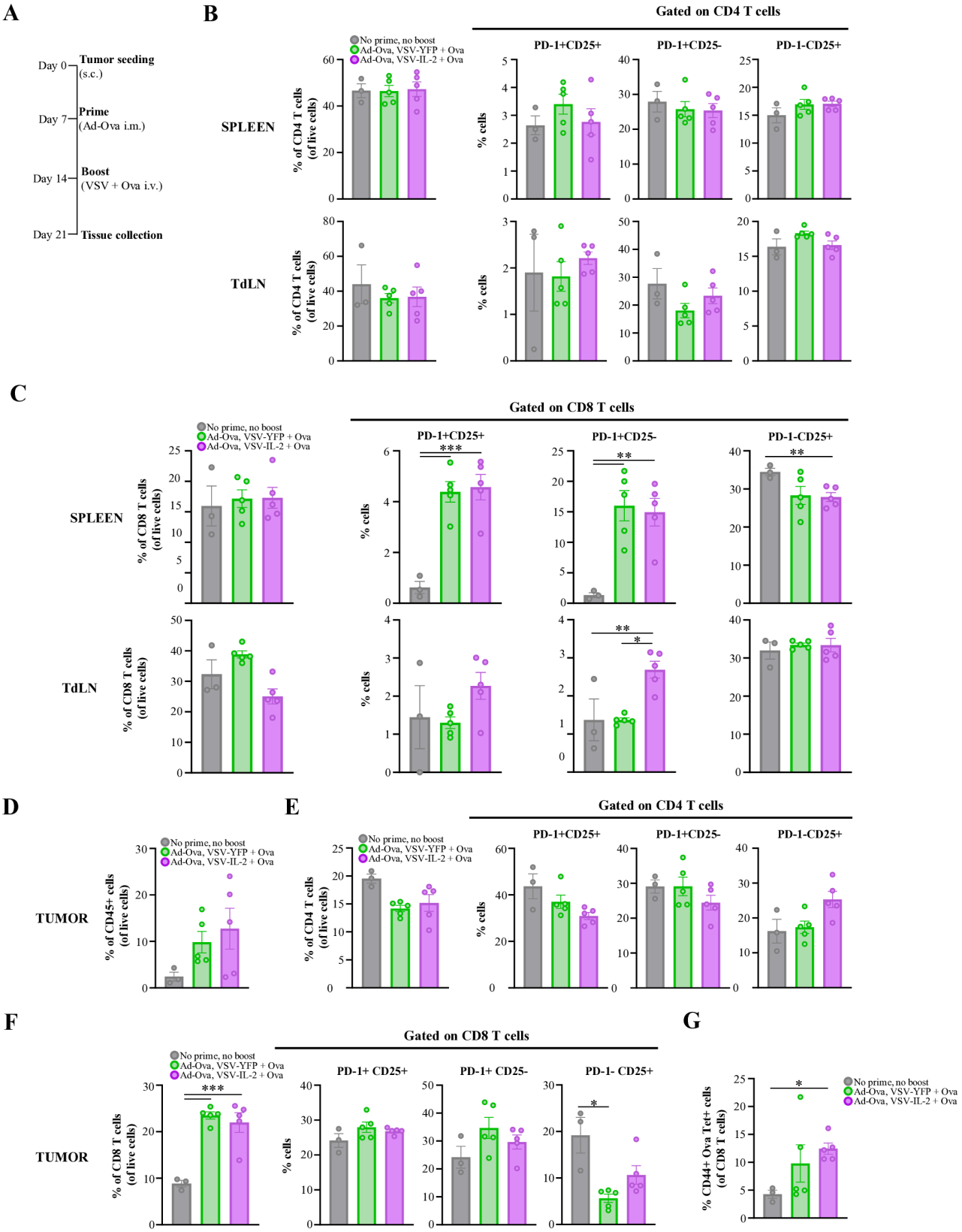

Figure 6 Adjuvant VSV-IL-2 boost enhances antigen-specific CD8 T cells in tumors without impacting T cells. (A) Schematic representation of the timeline used for prophylactic vaccination. (B) CD4 and (C) CD8 T cell analyses of immune cells extracted from the spleens and tumor-draining lymph nodes of B16F10-Ova tumor-bearing mice 7 days post-vaccination. (D) CD45+, (E) CD4+and (F) CD8+cell analyses from the tumors of the same mice. (G) % intratumoral CD8 T cells that are Ova Tet positive. (n=3 (PBS), 5 (VSV-YFP) and 5 (VSV-IL-2)). *p≤0.05, ***p≤0.001 (one-way analysis of variance with post hoc multiple comparison (B–G)). IL, interleukin; i.v., intravenous; Ova, ovalbumin; PBS, phosphate-buffered saline; PD-1, programmed cell death 1; TdLN, tumor-draining lymph node; VSV, vesicular stomatitis virus; YFP, yellow fluorescent protein.

in these tissues (figure 6B–F). Importantly, we also found that only VSV-IL-2-boosted mice had a statistically significant increase in Ova-specific CD8 T cells in their tumors (figure 6G). Altogether, our data show no differences in CD4 T-cell numbers and activation post-vaccination, but reveal increased intratumoral antigen-specific CD8 T cells with VSV-IL-2 vaccine adjuvant boost.

Therapeutic vaccination using VSV-IL-2 as an adjuvant improves CD8 effector functions and therapeutic efficacy

We next tested a therapeutic setting in which mice bearing established subcutaneous B16F10-Ova tumors are vaccinated (see experimental timeline in figure 7A). While this context is more clinically relevant compared with prophylactic vaccination, it does not allow for immune analyses over an extended period of time as most mice reach endpoint within 30 days. As we observed using the prophylactic model, we once again detected a strong induction of Ova tetramer+CD8 T cells in all vaccinated mice (figure 7B). In this therapeutic context, the levels of Ova-specific CD8 T cells were similar between both vaccinated groups at all time points. When analyzing the effector subsets of antigen-specific cells, we found increased levels of MPECs 7 days post-vaccination with VSV-IL-2, as we observed in the prophylactic setting, but this difference was lost by day 28 (figure 7C). Next, we evaluated the effector function of Ova-specific CD8 T cells induced by therapeutic VSV-IL-2 adjuvant vaccination boost. Interestingly, although no differences were observed in the proportions of IFN-γ+ and TNF-α+ CD8 T cells at days 21 and 28, a higher proportion of cytokine-producing CD8 T cells were found in the blood of the VSV-IL-2 cohort at day 35 (figure 7D). We then characterized these cytokine-producing cells. Although no differences were observed for the proportion of Tem and Tcm between both groups (online supplemental figure 5A), this time we observed significantly more SLECs, less MPECs and more DPECs 7 days post-vaccination (figure 7E).

Finally, we evaluated the therapeutic efficacies of the vaccines. Interestingly, VSV-IL-2-vaccinated mice had better tumor control and prolonged survival compared with their VSV-YFP-treated counterparts (figure 7F,G). A Pearson's analysis conducted between the survival time and the frequency of circulating cytokine-positive cells for each mouse revealed that the therapeutic efficacy of the vaccine correlated with the proportion of cytokine-producing CD8 T cells at days 21 and 28 (figure 7H). A positive, but not significant, correlation was also obtained at day 35 (online supplemental figure 5B). Notably, only two or three mice per group were still alive and analyzed at this later time point.

Overall, our results show that VSV-IL-2 adjuvant vaccination confers a therapeutic advantage over the parental virus, which correlates with the magnitude of Ova-specific CD8 T-cell effector functions.

DISCUSSION

We have previously shown that OVs are effective vaccination adjuvants when co-administered with antigenic peptides.[18] A major advantage of this vaccination platform against cancer is that the virus directly kills cancer cells. Also, the use of OVs as adjuvants offers a highly tailorable platform that allows for personalized vaccine formulations. In this study, we show that adjuvant OV vaccines can be further improved by using engineered viruses with enhanced immune-stimulating potential. More specifically, we demonstrated that VSV-IL-2 has improved vaccination adjuvanticity by both increasing the amount of antigen-specific MPECs, as well as by enhancing effector cytokine production.

The VSV-IL-2 variant has similar killing abilities compared with the parental virus and improves therapeutic efficacy only when used as an immune-boosting adjuvant. While we detected increased numbers of cytokine-producing T cells 3 weeks post-boost in tumor-bearing mice with VSV-IL-2, we observed this difference as early as 7 days post-boost in a tumor-free setting. This could be explained by the virus stimulating the immune system better in the context of sustained infection (with tumors), which would allow for the parental VSV-YFP to confer an improved boost, similar to that of VSV-IL-2. As such, differences between the two viruses would only be observed when the T-cell responses fade, which requires more than 1 week after vaccination. As such, vaccination in the context of cancer would confer a better early response and using VSV-IL-2 would allow for this response to be maintained longer. We also observed increased MPEC/SLEC ratios in the blood and increased antigen-specific CD8 T cells in the tumors of VSV-IL-2-boosted animals. Further work will investigate if these differences are driving the improved vaccine boost efficacy of VSV-IL-2 compared with VSV-YFP.

Using VSV as a vector for the expression of IL-2 confers multiple advantages over the systemic administration of the cytokine. First, IL-2 has a short serum half-life and thus requires frequent infusions in order to maintain effective systemic levels.[25 26] VSV-IL-2 would overcome this limitation by allowing infected cells to locally produce the cytokine for the duration of infection. Moreover, given that the virus preferentially targets cancer cells, IL-2 expression would theoretically be concentrated into the tumor niche using this approach, therefore allowing for high levels of the cytokine within the tumor microenvironment, while limiting its systemic expression and toxicity.[27] In line with this, we did not observe any adverse effects after treatment, therefore demonstrating that it was well tolerated.

Another essential aspect to consider is the impact of IL-2 on the activity and survival of regulatory T cells (Treg). Tregs constitutively express the high-affinity IL-2 receptor subunit α (CD25) and are therefore highly sensitive to the cytokine.[28] It has been reported that CD25 expression allows Tregs to sequester IL-2 and, as a consequence, prevents the activation of effector T cells (Teff).[29]

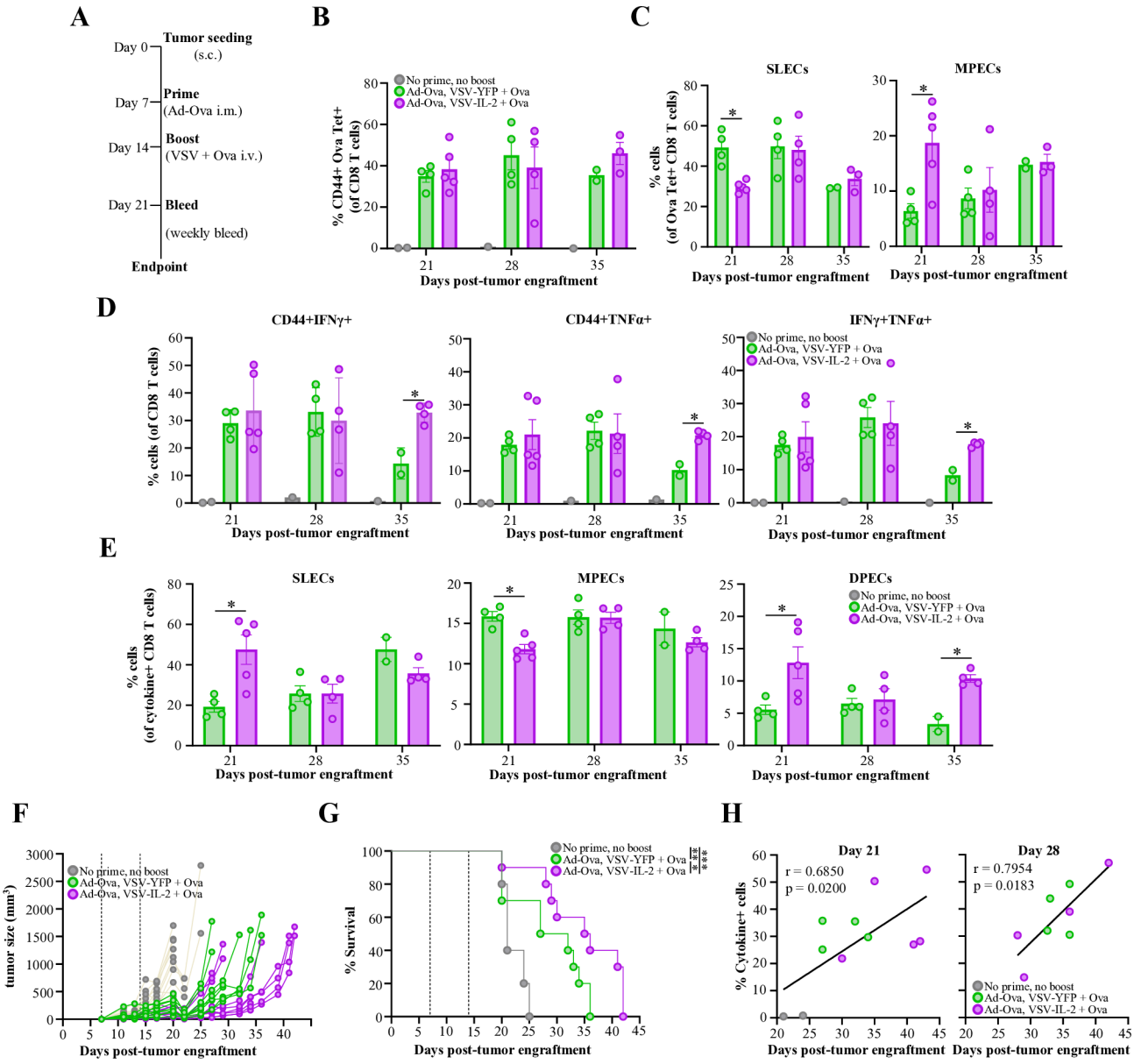

Figure 7 Adjuvant VSV-IL-2 boosting improves the therapeutic efficacy of the heterologous virus prime-boost vaccine. (A) Schematic representation of the timeline used for the therapeutic vaccination model. Percentages of (B) CD44+Ova Tet+ (C) SLECs and MPECs and (D) CD44+IFN-γ+, CD44+TNF-α+ and IFN-γ+TNF-α+ CD8T cells from blood collected at various time points post-therapeutic vaccination. (E) Proportions of SLECs, MPECs and DPECs (KLRG1+CD127+) within the cytokine-producing OVA-specific CD8 T cells. (F) Tumor growth curves and (G) Kaplan-Meier analysis of B16F10 tumor-bearing mice therapeutically vaccinated as depicted in a. (H) Pearson's correlation analysis between mouse survival time and the proportion of cytokine-producing OVA-specific CD8 T cells at days 21 and 28 post-tumor seeding after ex vivo restimulation. For immune analyses, n=2 (PBS), 4 (VSV-YFP) and 5 (VSV-IL2) at day 21, 1 (PBS), 4 (VSV-YFP) and 4 (VSV-IL-2) at day 28 and 1 (PBS), 2 (VSV-YFP) and 3 (VSV-IL-2) at day 35. For tumor growth and survival curves, n=5 for PBS and 10 for VSV-YFP and VSV-IL-2 groups. *p≤0.05 (one-way analysis of variance with post hoc multiple comparison between vaccinated groups (B, D), non-parametric t-test (C, E), Mantel-Cox (G), Pearson's correlation (H)). DPECs, double-positive effectors; IFN, interferon; IL, interleukin; i.m., intramuscular; i.v., intravenous; MPECs, memory precursor effector cell; Ova, ovalbumin; PBS, phosphate-buffered saline; s.c., subcutaneous; SLECs, short-lived effector cell; TNF, tumor necrosis factor; VSV, vesicular stomatitis virus; YFP, yellow fluorescent protein.

Given that we observed a strong antigen-specific CD8 T-cell response using VSV-IL-2, we believe that this effect was negligible in our system. Interestingly, high levels of IL-2 have been shown to trigger the functions of Teffs, while low levels promote the induction and proliferation of Tregs.[26 30] In our case, the virus is expected to produce high levels of IL-2 within the tumor niche, which would, as we observed, favor the activation of Teff cells. Nonetheless, future studies will investigate the impact of VSV-IL-2 on Tregs, as well as Treg activity and blockade in both vaccination regimens.

Acute exposure to high levels of IL-2 has previously been shown to limit the differentiation of CD8 T cells and favor a memory phenotype.[31] This is in line with our data that show the induction of more antigen-specific MPECs following prophylactic vaccination with VSV-IL-2. The increased levels of MPECs observed with our vaccine are highly desirable since these cells have better self-renewal capacities compared with SLECs and can ultimately become long-term Tcm cells.[31] Thus, VSV-IL-2 might also induce a better recall response compared with the parental virus.

In contrast, we observed the opposite phenotype in therapeutic vaccination, with more SLECs and fewer MPECs induced following boosting with VSV-IL-2. This discrepancy between the two models can be attributed to the presence of tumors during the therapeutic vaccination in comparison to the prophylactic setting. This tumor microenvironment likely drives CD8 T cells to adopt a more pronounced SLECs phenotype due to sustained inflammatory and antigenic signals.[32] Interestingly, however, this environment may also foster immunosuppressive populations, which could negatively impact the extent of the antigen-specific immune response. This might explain why we did not observe a difference in the frequency of antigen-specific CD8 T cells between the two vaccination groups in the therapeutic setting.

In the therapeutic setting, we also observed improved tumor control in VSV-IL-2-vaccinated mice. Interestingly, we found the proportion of antigen-specific CD8 T cells producing IFN-γ and TNF-α in response to Ova restimulation to correlate with survival. Among these, we observed a significant increase in the proportion of DPECs. Compared with MPECs, some DPECs have been shown to become "ex-KLRG1" memory cells that have both increased proliferation and cytotoxic capacities.[33] This might partially explain the longer-lasting effector functions exhibited by the tumor-specific CD8 T cells in VSV-IL-2-vaccinated mice.

Interestingly, we measured decreased levels of VSV-specific cells on VSV-IL-2 vaccine adjuvant boost, but not when using VSV-IL-2 as a direct therapy. This suggests that the vaccine, in conjunction with IL-2, detracts the immune response from VSV. Future work will investigate if this effect is also observed with other antigenic peptides when using VSV-IL-2 as a boosting adjuvant as this could have multiple benefits such as allowing for additional virus infusions, a limitation that currently restricts the dosing regimen.

Although we demonstrated that IL-2 is an interesting virally-encoded transgene candidate to improve vaccination, other pro-inflammatory mediators could also be effective. One of the main advantages of this adjuvant vaccination platform is its high flexibility, allowing for the use of different OVs as desired. For example, IL-7 and IL-15 have both been shown to be more effective adjuvants compared with IL-2 in the context of breast adenocarcinoma.[34] Another interesting candidate would be IFN-γ. We have previously engineered and described the VSV-IFN-γ OV variant, which we found enhanced dendritic cell maturation and antigenic presentation[17] when used as a direct treatment. In a vaccination context, the virus could potentially have increased adjuvanticity. Our approach would also allow for the co-administration of multiple cytokine-encoding VSV variants, potentially combining the benefits of each transgene in order to maximize the immune response. Future studies will investigate additional engineered OVs alone or in combination in the vaccination adjuvant prime-boost setting.

Altogether, we show that OVs that are modified to encode cytokines can be used as vaccination adjuvants to shape the anticancer immune response towards desired phenotypes. Our study provides a proof of concept that the vaccine adjuvant ability of OVs can be enhanced by transgene expression.

Acknowledgements We thank the NIH Tetramer Core Facility (contract number 75N93020D00005) for providing the MHC monomers and the team of Dr Nathalie Labrecque (IRCM) for the tetramerization protocol. Finally, we would like to thank the CRCHUM's Animal Facility for technical assistance.

Contributors VM-D designed and conducted experiments, analyzed and interpreted data, created the figures and wrote the manuscript. M-LM performed killing assays. AB, KG, MJRP, DB and KLD contributed to in vivo experiments. DGR contributed to the study design and edited the manuscript. M-CB-D: designed the project, created the virus, analyzed the data and wrote the manuscript. M-CB-D is the guarantor of this study.

Funding This work was supported by scholarships from the Quebec government's "Fonds de recherche du Québec en santé" (FRQS) (VM-D, KG, DB), the "Université de Montréal" (VM-D, DB), the CRCHUM (AB and KG) and the "Institut du cancer de Montréal" (VM-D, M-LM, AB, KG, MJRP, DB). M-CB-D received salary awards from the FRQS and the Quebec Breast Cancer Foundation and DGR from the FRQS. This project was funded by the "Institut du cancer de Montréal".

Competing interests None declared.

Patient consent for publication Not applicable.

Ethics approval All in vivo experiments were conducted in accordance with the CRCHUM's animal care committee (C22019MCBDs).

Provenance and peer review Not commissioned; externally peer reviewed.

Data availability statement All data relevant to the study are included in the article or uploaded as supplementary information.

ORCID iD

Marie-Claude Bourgeois-Daigneault http://orcid.org/0000-0002-9091-2235

REFERENCES

1 Ilkow CS, Swift SL, Bell JC, *et al*. From scourge to cure: tumour-selective viral pathogenesis as a new strategy against cancer. *PLoS Pathog* 2014;10:e1003836.
2 Guo ZS, Liu Z, Bartlett DL. Oncolytic Immunotherapy: Dying the Right Way is a Key to Eliciting Potent Antitumor Immunity. *Front Oncol* 2014;4:74.
3 Kaufman HL, Kohlhapp FJ, Zloza A. Oncolytic viruses: a new class of immunotherapy drugs. *Nat Rev Drug Discov* 2015;14:642–62.
4 Melcher A, Harrington K, Vile R. Oncolytic virotherapy as immunotherapy. *Science* 2021;374:1325–6.
5 Aitken AS, Roy DG, Bourgeois-Daigneault MC. Taking a Stab at Cancer; Oncolytic Virus-Mediated Anti-Cancer Vaccination Strategies. *Biomedicines* 2017;5:3.
6 Bridle BW, Stephenson KB, Boudreau JE, *et al*. Potentiating cancer immunotherapy using an oncolytic virus. *Mol Ther* 2010;18:1430–9.
7 Bridle BW, Clouthier D, Zhang L, *et al*. Oncolytic vesicular stomatitis virus quantitatively and qualitatively improves primary CD8$^+$ T-cell responses to anticancer vaccines. *Oncoimmunology* 2013;2:e26013.
8 Pol JG, Zhang L, Bridle BW, *et al*. Maraba virus as a potent oncolytic vaccine vector. *Mol Ther* 2014;22:420–9.
9 Aitken AS, Roy DG, Martin NT, *et al*. Brief Communication; A Heterologous Oncolytic Bacteria-Virus Prime-Boost Approach for Anticancer Vaccination in Mice. *J Immunother* 2018;41:125–9.
10 Pol JG, Atherton MJ, Stephenson KB, *et al*. Enhanced immunotherapeutic profile of oncolytic virus-based cancer vaccination using cyclophosphamide preconditioning. *J Immunother Cancer* 2020;8:e000981.
11 Simovic B, Walsh SR, Wan Y. Mechanistic insights into the oncolytic activity of vesicular stomatitis virus in cancer immunotherapy. *Oncolytic Virother* 2015;4:157–67.
12 Stojdl DF, Lichty BD, tenOever BR, *et al*. VSV strains with defects in their ability to shutdown innate immunity are potent systemic anti-cancer agents. *Cancer Cell* 2003;4:263–75.
13 Bright R, Coventry BJ, Eardley-Harris N, *et al*. Clinical Response Rates From Interleukin-2 Therapy for Metastatic Melanoma Over 30 Years' Experience: A Meta-Analysis of 3312 Patients. *J Immunother* 2017;40:21–30.
14 Fishman M, Dutcher JP, Clark JI, *et al*. Overall survival by clinical risk category for high dose interleukin-2 (HD IL-2) treated patients with metastatic renal cell cancer (mRCC): data from the PROCLAIM^{SM} registry. *J Immunother Cancer* 2019;7:84.
15 Dutcher JP, Schwartzentruber DJ, Kaufman HL, *et al*. High dose interleukin-2 (Aldesleukin) - expert consensus on best management practices-2014. *J Immunother Cancer* 2014;2:26.
16 Roy DG, Power AT, Bourgeois-Daigneault MC, *et al*. Programmable insect cell carriers for systemic delivery of integrated cancer biotherapy. *J Control Release* 2015;220:210–21.
17 Bourgeois-Daigneault M-C, Roy DG, Falls T, *et al*. Oncolytic vesicular stomatitis virus expressing interferon-γ has enhanced therapeutic activity. *Mol Ther Oncolytics* 2016;3:16001.
18 Roy DG, Geoffroy K, Marguerie M, *et al*. Adjuvant oncolytic virotherapy for personalized anti-cancer vaccination. *Nat Commun* 2021;12:2626.
19 Lin JX, Leonard WJ. The role of Stat5a and Stat5b in signaling by IL-2 family cytokines. *Oncogene* 2000;19:2566–76.
20 Bridle BW, Hanson S, Lichty BD. Combining oncolytic virotherapy and tumour vaccination. *Cytokine Growth Factor Rev* 2010;21:143–8.
21 Rajwani J, Vishnevskiy D, Turk M, *et al*. VSVΔM51 drives CD8+ T cell-mediated tumour regression through infection of both cancer and non-cancer cells. *Nat Commun* 2024;15:9933.
22 Rötzschke O, Falk K, Stevanović S, *et al*. Exact prediction of a natural T cell epitope. *Eur J Immunol* 1991;21:2891–4.
23 Koh CH, Lee S, Kwak M, *et al*. CD8 T-cell subsets: heterogeneity, functions, and therapeutic potential. *Exp Mol Med* 2023;55:2287–99.
24 Le CT, Vick LV, Collins C, *et al*. Regulation of human and mouse bystander T cell activation responses by PD-1. *JCI Insight* 2023;8:e173287.
25 Donohue JH, Rosenberg SA. The fate of interleukin-2 after in vivo administration. *J Immunol Baltim Md* 1950;130:2203–8.
26 Raeber ME, Sahin D, Karakus U, *et al*. A systematic review of interleukin-2-based immunotherapies in clinical trials for cancer and autoimmune diseases. *EBioMedicine* 2023;90:104539.
27 Sun Z, Ren Z, Yang K, *et al*. A next-generation tumor-targeting IL-2 preferentially promotes tumor-infiltrating CD8$^+$ T-cell response and effective tumor control. *Nat Commun* 2019;10:3874.
28 Ross SH, Cantrell DA. Signaling and Function of Interleukin-2 in T Lymphocytes. *Annu Rev Immunol* 2018;36:411–33.
29 Chinen T, Kannan AK, Levine AG, *et al*. An essential role for the IL-2 receptor in Treg cell function. *Nat Immunol* 2016;17:1322–33.
30 Yu A, Snowhite I, Vendrame F, *et al*. Selective IL-2 responsiveness of regulatory T cells through multiple intrinsic mechanisms supports the use of low-dose IL-2 therapy in type 1 diabetes. *Diabetes* 2015;64:2172–83.
31 Kalia V, Sarkar S. Regulation of Effector and Memory CD8 T Cell Differentiation by IL-2-A Balancing Act. *Front Immunol* 2018;9:2987.
32 Joshi NS, Cui W, Chandele A, *et al*. Inflammation directs memory precursor and short-lived effector CD8(+) T cell fates via the graded expression of T-bet transcription factor. *Immunity* 2007;27:281–95.
33 Herndler-Brandstetter D, Ishigame H, Shinnakasu R, *et al*. KLRG1+ Effector CD8+ T Cells Lose KLRG1, Differentiate into All Memory T Cell Lineages, and Convey Enhanced Protective Immunity. *Immunity* 2018;48:716–29.
34 Cha E, Graham L, Manjili MH, *et al*. IL-7 + IL-15 are superior to IL-2 for the ex vivo expansion of 4T1 mammary carcinoma-specific T cells with greater efficacy against tumors in vivo. *Breast Cancer Res Treat* 2010;122:359–69.